PRIMARY RESEARCH ARTICLE

WILEY ·Global Change Biology

Biotic responses buffer warming-induced soil organic carbon loss in Arctic tundra

Junyi Liang[1,2] (ID) | **Jiangyang Xia**[3,4] (ID) | **Zheng Shi**[1] (ID) | **Lifen Jiang**[1,5] | **Shuang Ma**[1,5] | **Xingjie Lu**[1,5] (ID) | **Marguerite Mauritz**[5] (ID) | **Susan M. Natali**[6] | **Elaine Pegoraro**[5] | **Christopher Ryan Penton**[7,8] | **César Plaza**[5,9,10] | **Verity G. Salmon**[2] (ID) | **Gerardo Celis**[5] | **James R. Cole**[11] | **Konstantinos T. Konstantinidis**[12] | **James M. Tiedje**[11] | **Jizhong Zhou**[1,13,14,15] | **Edward A. G. Schuur**[5] | **Yiqi Luo**[1,5,16]

[1]Department of Microbiology and Plant Biology, University of Oklahoma, Norman, Oklahoma

[2]Environmental Sciences Division and Climate Change Science Institute, Oak Ridge National Laboratory, Oak Ridge, Tennessee

[3]Tiantong National Station of Forest Ecosystem, Research Center for Global Change and Ecological Forecasting, School of Ecological and Environmental Sciences, East China Normal University, Shanghai, China

[4]Institute of Eco-Chongming (IEC), Shanghai, China

[5]Center for Ecosystem Science and Society and Department of Biological Sciences, Northern Arizona University, Flagstaff, Arizona

[6]Woods Hole Research Center, Falmouth, Massachusetts

[7]College of Integrative Sciences and Arts, Arizona State University, Mesa, Arizona

[8]Center for Fundamental and Applied Microbiomics, Biodesign Institute, Arizona State University, Tempe, Arizona

[9]Departamento de Biología y Geología, Física y Química Inorgánica, Escuela Superior de Ciencias Experimentales y Tecnología, Universidad Rey Juan Carlos, Móstoles, Spain

[10]Instituto de Ciencias Agrarias, Consejo Superior de Investigaciones Científicas, Madrid, Spain

[11]Department of Plant, Soil and Microbial Sciences, Center for Microbial Ecology, Michigan State University, East Lansing, Michigan

[12]School of Civil and Environmental Engineering and School of Biology, Georgia Institute of Technology, Atlanta, Georgia

[13]Institute for Environmental Genomics, University of Oklahoma, Norman, Oklahoma

[14]State Key Joint Laboratory of Environment Simulation and Pollution Control, School of Environment, Tsinghua University, Beijing, China

[15]Earth and Environmental Sciences, Lawrence Berkeley National Laboratory, Berkeley, California

[16]Department of Earth System Science, Tsinghua University, Beijing, China

Correspondence
Junyi Liang and Yiqi Luo, Department of Microbiology and Plant Biology, University of Oklahoma, Norman 73019, OK.
Emails: liangj@ornl.gov (J. L.); Yiqi.Luo@nau.edu (Y. L.)

Abstract

Climate warming can result in both abiotic (e.g., permafrost thaw) and biotic (e.g., microbial functional genes) changes in Arctic tundra. Recent research has incorporated dynamic permafrost thaw in Earth system models (ESMs) and indicates that Arctic tundra could be a significant future carbon (C) source due to the enhanced decomposition of thawed deep soil C. However, warming-induced biotic changes may influence biologically related parameters and the consequent projections in ESMs. How model parameters associated with biotic responses will change under warming and to what extent these changes affect projected C budgets have not been carefully examined. In this study, we synthesized six data sets over 5 years from a soil warming experiment at the Eight Mile Lake, Alaska, into the Terrestrial ECOsystem (TECO) model with a probabilistic inversion approach. The TECO model used multiple soil layers to track dynamics of thawed soil under different

treatments. Our results show that warming increased light use efficiency of vegetation photosynthesis but decreased baseline (i.e., environment-corrected) turnover rates of SOC in both the fast and slow pools in comparison with those under control. Moreover, the parameter changes generally amplified over time, suggesting processes of gradual physiological acclimation and functional gene shifts of both plants and microbes. The TECO model predicted that field warming from 2009 to 2013 resulted in cumulative C losses of 224 or 87 g/m^2, respectively, without or with changes in those parameters. Thus, warming-induced parameter changes reduced predicted soil C loss by 61%. Our study suggests that it is critical to incorporate biotic changes in ESMs to improve the model performance in predicting C dynamics in permafrost regions.

1 | INTRODUCTION

The enormous quantity of soil organic carbon (SOC) in Arctic ecosystems has long been protected due to low temperatures. As the climate warms, this SOC can become vulnerable, potentially releasing a large amount of carbon (C) to the atmosphere, thus acting as an important C source (Hicks Pries, Schuur, Natali, & Crummer, 2016; Koven et al., 2011; Macdougall, Avis, & Weaver, 2012; Schuur et al., 2009, 2015). However, the magnitude of these potential C losses remains uncertain due to a poor understanding of the underlying mechanisms that control the soil C balance in these Arctic ecosystems (Koven, Riley, & Stern, 2013; Mcguire et al., 2012, 2016).

Climate warming can influence the soil C balance in Arctic ecosystems through various mechanisms. First, temperature increases can directly stimulate soil C release due to the thermal kinetic behavior of microbial-mediated processes (Bracho et al., 2016; Davidson & Janssens, 2006; Liang et al., 2015). Second, permafrost thaw can increase SOC accessibility for decomposers by lifting temperature and moisture constraints (i.e., thawing permafrost and increasing soil drainage), potentially resulting in more C release from Arctic ecosystems to the atmosphere (Hicks Pries et al., 2016; Koven et al., 2011; Schuur et al., 2009). In Earth system models (ESMs), the direct impact of a temperature increase on SOC decomposition is usually reflected by temperature sensitivity (e.g., Oleson et al., 2013). Recently, permafrost thaw has also been incorporated into the model by using a multilayer soil structure (e.g., Koven et al., 2011). The inclusion of permafrost thaw into these models results in the availability of additional previously frozen SOC for decomposition and therefore predict that Arctic ecosystems may become significant C sources by the end of this century and beyond (Koven, Lawrence, & Riley, 2015; Koven et al., 2011; Schuur et al., 2015).

However, the current generation of models generally does not account for biological adjustments when ecosystems are exposed to different environmental conditions. ESMs usually use scenario-invariant constants as parameters to represent processes at multiple scales. For example, the turnover rate of a SOC pool is a representation of many processes related to decomposing the SOC pool. Some of the processes, such as the lability of the SOC pool, can be explicitly represented by model structure of multiple pools at the resolved scales. However, other processes, such as the composition of microbial taxa, microbial richness, and microbial activity, which collectively represent the ability of microbial community to decompose SOC, have not been explicitly represented in models yet. Those biological processes that operate on unresolved scales need to be implicitly represented in models by parameterization for their interactions with processes at the resolved scales (Bauer, Thorpe, & Brunet, 2015; Shi et al., 2015; Xu, White, Hui, & Luo, 2006).

Recent observational studies have shown that warming and permafrost thaw can influence microbial community composition and activity in Arctic ecosystems (Hultman et al., 2015; Manzoni, Taylor, Richter, Porporato, & Ågren, 2012; Xue et al., 2016). These changes may lead to alterations in SOC pool turnover rates but have not been well explored by ESMs. Before we develop the capability to explicitly represent those microbial changes at the resolved scales, they usually can be represented by changes in parameter values. Such environment-induced parameter changes have been found in other ecosystems (Shi et al., 2015; Xu et al., 2006). However, how biological properties may be influenced by increases in temperature and permafrost thaw, and the consequent influences on the prediction of C pools and flux, are still not clear in the vulnerable Arctic ecosystems.

Data assimilation, which allows incorporating multisourced data into models, has increasingly been used to estimate model parameter values (Keenan, Davidson, Munger, & Richardson, 2013; Luo et al., 2016; Shi et al., 2015; Williams et al., 2009; Xu et al., 2006). Data assimilation may help understand the C cycle and its feedback to climate change in at least two ways. First, models usually perform

better after data assimilation, exhibiting a higher degree of fit between observations and model output (Bauer et al., 2015; Shi et al., 2015; Williams et al., 2009; Xu et al., 2006). Second, detected changes in model parameters under different scenarios may be used to reveal changes in processes at the unresolved scales, which are difficult to either directly measure using experimental techniques or explicitly represented in model structure or both (Luo et al., 2011, 2016).

A long-term field warming manipulative experiment has been conducted in an Arctic tundra (Natali, Schuur, & Rubin, 2012; Natali, Schuur, Webb, Pries, & Crummer, 2014; Natali et al., 2011). In the current study, we attempted to quantify warming-induced changes in model parameters associated with biological properties in the Arctic tundra by integrating data from the experiment and a process-based model. In addition to revealing the dependence of the parameter changes on treatment year, we explored how the altered parameters influence the estimation of soil C loss in the Arctic tundra.

2 | MATERIALS AND METHODS

2.1 | Experimental design

The Carbon in Permafrost Experimental Heating Research (CiPEHR) experiment was established at a moist acidic tundra in the region of Eight Mile Lake (EML), Alaska, USA (63°52′59″N, 149°13′32″W) in 2008 (Natali et al., 2011). Site information, experimental design and field observations are described in detail in previous publications (Mauritz et al., 2017; Natali et al., 2011, 2012, 2014). Briefly, the site lies within the area of discontinuous permafrost, with an active layer depth of approximately 50 cm at the beginning of the experiment. Mean annual temperature and precipitation are −1.0°C and 378 mm, respectively. The lowest and highest mean monthly temperatures are −16°C in December and 15°C in July (Schuur et al., 2009).

In the experiment, soil was warmed by six replicate snow fences in three blocks that accumulate snow during the winter months, thus serving as an insulator. The excess snow and fences were removed from the warming plots before snow melt in early spring to ensure comparable melt out dates and snow water input across treatments. The experimental treatment started in September 2008, and continued every winter. During 2009–2013, the experimental treatment increased soil temperatures by ~0.9°C across the layers of 0–40 cm, increased soil moisture by 4.2% (V/V), and increased thaw depth by 12.5% (Salmon et al., 2016). Gross Primary Production (GPP), Ecosystem Respiration (ER), Net Ecosystem CO_2 Exchange (NEE), soil C stocks, and aboveground and belowground biomass in both the ambient and warming treatments were used for parameter estimation in the model as described below.

2.2 | Model

The Terrestrial ECOsystem (TECO) model was used in this study. In the model, GPP was simulated by

$$GPP(t) = PAR(t) \times FAPAR(t) \times LUE \times \tau(t)$$

where PAR is photosynthetic active radiation ($\mu E\ m^{-2}\ s^{-1}$), which is derived from a weather station located approximately 100 m from the experiment. FAPAR is the fraction of absorbed PAR by plants, which is Moderate Resolution Imaging Spectroradiometer (MODIS) Normalized Difference Vegetation Index (NDVI) in the grid cell which the experiment site is in. In situ measurements showed that warming increased NDVI by 6.8% (Natali et al., 2012). Thus, a factor of 1.068 was applied to FAPAR in the warming treatment. LUE is light use efficiency (g C ($\mu E\ m^{-2}\ s^{-1})^{-1}$), which was determined by data assimilation described below. τ is environmental scaler.

Carbon dynamics within the ecosystem were modeled according to Luo, Wan, Hui, and Wallace (2001), Luo et al. (2017) as:

$$\frac{dX(t)}{dt} = B \times GPP(t) + \xi \times A \times K \times X(t),$$

where $X(t)$ is a 15 × 1 vector describing C pool sizes (i.e., two plant pools, one litter pool, four soil layers with three soil pools in each layer) at time t. $B = [b_{shoot}\ b_{root}\ 0\ 0\ 0\ 0\ 0\ 0\ 0\ 0\ 0\ 0\ 0\ 0\ 0]^T$ is a vector describing GPP allocations to the C pools. GPP only directly allocates to shoots (b_{shoot}), roots b_{root} and autotrophic respiration ($1-b_{shoot}-b_{root}$). A is a square matrix representing C transfers between individual C pools (black arrows in Figure 1). All the diagonal elements in the matrix A are −1. K is a diagonal matrix representing pool turnover rates (the amount of C per unit mass leaving each of the pools per time step). ξ is environmental scaler. A detailed description on the matrix presentation of the terrestrial C dynamics model can be found in Luo et al. (2017). In the model, the C dynamic is dependent on active layer thickness (ALT; Figure 1). Only pools in the active layer are involved at each time step.

2.3 | Gap-filling ALT

To obtain daily values of ALT for this analysis, we fit a linear function between ALT and a metric of air temperature during the thawing period. This metric, cumulative air temperature (T_{cum}), is defined as accumulated degree-days above 0°C. In each spring, when the air temperature over seven continuous days was >0°C, the first day of the 7 days was marked as the start of the thawing period. In each fall, when air temperatures over seven continuous days were below 0°C, the day before the first day of the 7 days was marked as the end of the thawing period. T_{cum} was calculated during the thawing period from monitored air temperature. With the calculated T_{cum}, ALT is computed by

$$ALT = aT_{cum} + b,$$

where a and b are parameters, and were determined using linear regression. During the freeze-up period, we adopted the seasonal pattern of the simulated ALT in both the control and warming scenarios in the Community Land Model version 4.5 (CLM 4.5) in the grid where the CiPEHR site is, and modified it based on the measured maximum ALT by multiplying a factor between 1/5 and 1/3.5
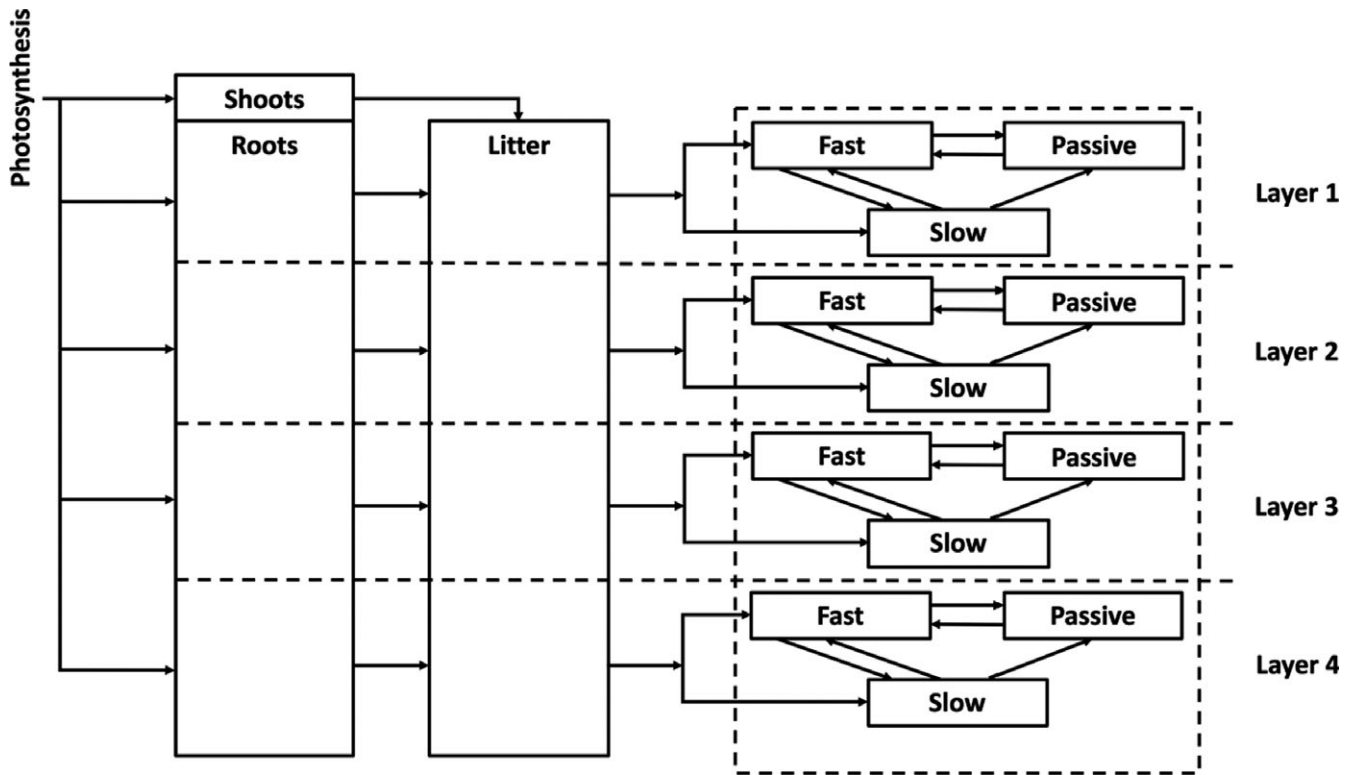
FIGURE 1 Model structure with two plant pools, one litter pool, and four soil layers with three soil pools in each layer. Active layer thickness varies over time. Only pools in the active layer are involved at each time step

depending on the treatment and year. A minimum ALT of 0.5 cm was set to represent soil C availability during the winters.

2.4 | Parameters to be constrained

Previous studies have shown that in transient systems, data assimilation can provide more reasonable model initial conditions, compared to prescribed inputs (Carvalhais et al., 2008; Williams et al., 2009). In this study, the initial pool sizes of plant shoots, roots, litter, fast soil, slow soil, and passive soil pools, were constrained using data in the ambient treatment. The constrained initial pools in the ambient treatment were also used in the warming treatment, assuming that no significant difference existed between the ambient and warming treatment before the treatment started.

With these identical initial conditions, 16 parameters were estimated twice, respectively, in the ambient and warming treatments, using the data assimilation described below. These parameters include (1) light use efficiency (LUE) in the GPP model; GPP allocations to (2) shoots (b_{shoot}) and (3) roots (b_{root}) in the vector B; turnover rates of (4) shoots (k_{shoot}), (5) roots (b_{root}), (6) litter (k_{litter}), (7) fast soil C (k_{fast}), (8) slow soil C (k_{slow}), and (9) passive soil C ($k_{passive}$) in matrix K; C transfer coefficient from (10) litter to fast soil C ($a_{fast, litter}$), (11) from litter to slow soil C ($a_{slow,litter}$), (12) from fast soil C to slow soil C($a_{slow,fast}$), (13) from fast soil C to passive soil C ($a_{passive,fast}$), (14) from slow soil C to fast soil C ($a_{fast,slow}$), (15) from

slow soil C to passive soil C ($a_{passive,litter}$), and (16) from passive soil C to fast soil C ($a_{fast,passive}$).

2.5 | Data assimilation

A probabilistic inversion approach, based on Bayes' theorem, was used to constrain the model parameters (Xu et al., 2006):

$$P(\theta|Z) \propto P(Z|\theta)P(\theta),$$

where $P(\theta)$ is priori probability density function (PDF). $P(Z|\theta)$ is a likelihood function with the assumption that the model error follows a multivariate Gaussian distribution:

$$P(Z|\theta) \propto \exp\left\{-\sum_{i=1}^{6}\sum_{t\in\text{obs}(Z_i)}\frac{[Z_i(t)-X_i(t)]^2}{2\sigma_i^2(t)}\right\},$$

where $Z_i(t)$ and $X_i(t)$ are the observed and modeled values at time t, and $\sigma_i(t)$ is the standard deviation of measurements. The value of i from 1 to 6 denotes GPP, ER, NEE, aboveground and belowground biomass, and soil C, respectively (Table 1). $P(\theta|Z)$ is the posterior PDF, which is constrained by using adaptive Metropolis (AM) algorithm, a Markov Chain Monte Carlo (MCMC) technique (Haario, Saksman, & Tamminen, 2001; Hararuk, Xia, & Luo, 2014). In the AM algorithm, the proposal distribution at each iteration is estimated depending on the past iterations by setting a covariance matrix

TABLE 1 Data used for the parameterization

Data	Year	Period	Time step
Growing season NEE	2009–2013	May–September	Daily[a]
Growing season GPP	2009–2013	May–September	Daily[a]
Growing season ER	2009–2013	May–September	Daily[a]
Aboveground biomass	2009–2013		Yearly
Belowground biomass	2011		Yearly
Soil C	2009–2011, 2013		Yearly

Notes. ER, Ecosystem Respiration; GPP, Gross Primary Production; NEE, Net Ecosystem CO_2 Exchange.

[a]Daily data were calculated from half-hourly measurements to match the time step of the model.

$$C_i = \begin{cases} C_0, & i \leq i_0, \\ s_d cov(\theta_0, \cdots \theta_{i-1}) & i \leq i_0, \end{cases}$$

where s_d is a parameter calculated based on dimension d (i.e., $s_d = 2.38/\sqrt{d}$, and $d = 16$ in this study) (Gelman, Roberts, & Gilks, 1996; Hararuk et al., 2014). An arbitrary initial covariance C_0 is required in the AM algorithm when iteration is not greater than i_0 ($i_0 = 4,000$ in this study). C_0 is constructed by a test run in which the new parameter is selected by a random move from the previous one within a uniform distributed range (Hararuk et al., 2014; Liang et al., 2015; Xu et al., 2006). The boundaries of the uniform distribution are selected based on observations at the study site (Mauritz et al., 2017; Natali et al., 2011, 2012, 2014; Salmon et al., 2016; Webb et al., 2016) and published data assimilation papers (Shi et al., 2015; Weng & Luo, 2011) (Table 2).

The AM algorithm was run repeatedly for 50,000 iterations to derive the posterior PDF. The initial set of parameters was randomly selected within the priori parameter ranges. At each iteration, a set of parameters (θ^{new}) is proposed based on the accepted parameters in the previous iteration (θ^{old}) and C_i. Then the acceptance probability is calculated by

$$\alpha = \min\left\{1, \frac{P(Z|\theta^{new})P(\theta^{new})}{P(Z|\theta^{old})P(\theta^{old})}\right\}.$$

The acceptance probability is compared with a random number u between 0 and 1. If $\alpha > u$, the new set of parameters θ^{new} is accepted. Otherwise, θ^{new} is set to θ^{old}. The data assimilation was first applied to synthesizing all 5-year data to explore the overall effect of warming on parameters. Data of each year were used to estimate parameters respectively to reveal how the effect of warming on parameters may change with exposure time.

The model performance was tested by comparing the model simulations and observations. For GPP, ER, and NEE, the coefficient of determination (R^2) was used to evaluate the goodness-of-fit. Because R^2 is not suitable for assessing the goodness-of-fit regarding a small amount of data, we used the mean absolute percentage error (MAPE) to evaluate the model simulated biomass-C:

$$MAPE = \frac{100}{n} \sum_{i=1}^{n} \left| \frac{Y_{obs}(i) - Y_{sim}(i)}{Y_{obs}(i)} \right|$$

where Y_{obs} and Y_{sim} are observed and simulated values, respectively. A smaller MAPE means a better model simulation.

2.6 | Modeling experiments

With all the accepted parameter sets, the model was used to explore impacts of biotic responses on SOC loss at the permafrost site. We

TABLE 2 The boundaries of priori uniform distributions and the maximum likelihood estimates (MLEs) of the posterior probability functions of the focused 16 parameters

Parameter	Symbol	Priori Minimum	Priori Maximum	MLE Ambient	MLE Warming
Light use efficiency ($\times 10^{-1}$ g C (μE m^{-2} s^{-1})$^{-1}$)	LUE	0.01	0.10	0.68	0.85
GPP allocation to shoots	b_{shoot}	0.00	0.50	0.39	0.39
GPP allocation to roots	b_{root}	0.00	0.50	0.24	0.23
Turnover rate of shoots ($\times 10^{-2}$ day^{-1})	k_{shoot}	0.01	5.00	3.55	3.50
Turnover rate of roots ($\times 10^{-3}$ day^{-1})	k_{root}	0.10	5.00	4.70	4.80
Turnover rate of litter ($\times 10^{-3}$ day^{-1})	k_{litter}	1.00	10.00	7.70	7.60
Turnover rate of fast soil ($\times 10^{-3}$ day^{-1})	k_{fast}	0.10	5.00	1.45	1.25
Turnover rate of show soil ($\times 10^{-4}$ day^{-1})	k_{slow}	0.00	2.00	1.06	0.82
Turnover rate of passive soil ($\times 10^{-7}$ day^{-1})	$k_{passive}$	0.00	1.00	0.54	0.53
C transfer from litter to fast soil	$a_{fast,litter}$	0.10	0.50	0.12	0.12
C transfer from litter to slow soil	$a_{slow,litter}$	0.05	0.15	0.07	0.07
C transfer from fast to slow soil	$a_{slow,fast}$	0.10	0.50	0.31	0.31
C transfer from fast to passive soil	$a_{passive,fast}$	0.00	0.15	0.08	0.08
C transfer from slow to fast soil	$a_{fast,slow}$	0.10	0.50	0.32	0.32
C transfer from slow to passive soil	$a_{passive,slow}$	0.00	0.10	0.05	0.05
C transfer from passive to fast soil	$a_{fast,passive}$	0.10	0.50	0.29	0.29
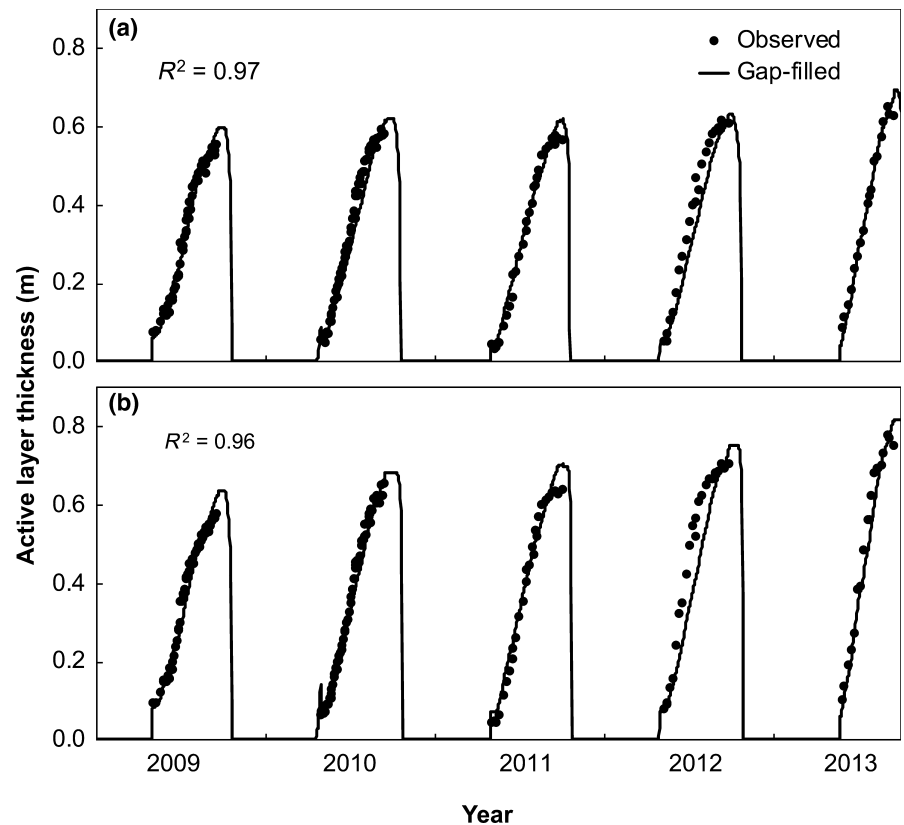
FIGURE 2 Gap-filled (lines) and observed (dots) active layer thickness in the ambient (a) and warming treatment (b)

acknowledge that the biotic responses as reflected in estimated parameter changes may be model-specific. The very parameters whose values were estimated to change under the warming treatments may be different when a different model was used. No matter which model would be used in data assimilation, it is very likely that parameter values have to adjust to match model with data well when the environment changes. It is because it is pervasive that the parameters have to be adjusted again in order to fit data well so as to reflect biotic properties in the new environment (Li et al., 2016).

In this study, the model was run forward in three scenarios. The first scenario was the control with physical forcings to influence temperature, ALT, and other physical processes in the ambient treatment with parameter sets constrained by data in the ambient treatment. The second scenario was for physical change without biotic responses to warming. In this scenario, we used physical forcings in the warming treatment with parameter sets constrained by data in the ambient treatment. The third scenario was to explore both physical change and biotic responses to soil warming. We used physical forcings in the warming treatment with parameter sets constrained by data in the warming treatment. By comparing the three scenarios, we explored how changes in parameters representing biological processes influence the C dynamic in the permafrost site.

3 | RESULTS

The fitted empirical function was able to simulate the ALT from cumulative air temperature, with an R^2 of 0.97 and 0.96 in the

ambient and the warming treatments, respectively (Figure 2). The values of the slope (a) and intercept (b) of the linear function were 3.58×10^{-4} and 0.035 in ambient, and 3.65×10^{-4} and 0.056 in warming, respectively. The modified ALT during the freeze-up showed longer zero-curtain period in the warming treatment than that in the ambient treatment (Figure 2). The calculated daily ALT (Figure 2) was input to drive the model.

In addition to the simulated ALT, we used observed soil temperature and soil moisture in both the control and warming treatments to drive the TECO model for both data assimilation and forward simulation. In this way, the abiotic changes were accounted for in this study. Out of the 16 parameters we explored, three were significantly changed by the warming treatment (Table 2, Figure 3). LUE, which represents the efficiency of energy transfer from absorbed PAR to GPP in the vegetation canopy, increased by 28.6% (Figure 3a) under warming in comparison with the control. Warming significantly reduced the baseline (i.e., environment-corrected) turnover rates of the fast and slow SOC pools (Figure 3b, c). Additionally, changes in those parameters were dependent on treatment year (Figure 4). The warming effect on LUE increased gradually in the five experimental years, with small fluctuations observed in 2013 (Figure 4a). Additionally, the decreased magnitude of the baseline turnover rate of the fast and slow SOC pools was amplified (Figure 4b, c). The warming effect on the baseline turnover rate of the fast SOC pool changed from −2.9% to −60.7% during 2009–2013 (Figure 4b), while the warming effect on the baseline turnover rate of the slow SOC pool decreased from 9.8% to −31.0% (Figure 4c).
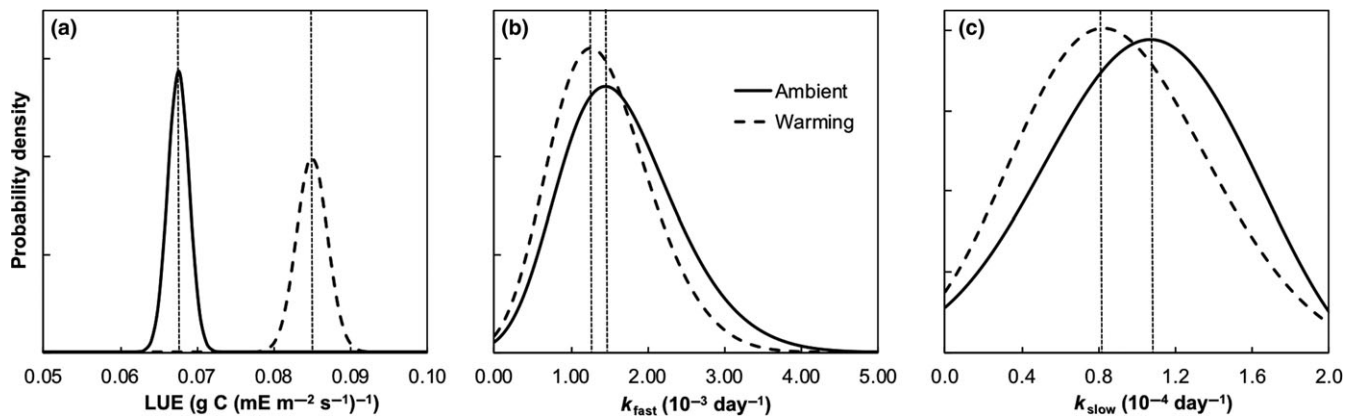
FIGURE 3 Effect of warming on the probability distribution of parameters. (a) light use efficiency; (b) baseline (i.e., environment-corrected) turnover rate of the fast SOC pool (k_{fast}); (c) baseline turnover rate of the slow SOC pool (k_{slow}). The solid and dashed lines are the parameter distributions of the ambient and warming treatment, respectively. The vertical dotted lines are to denote the maximum likelihood estimates of parameters
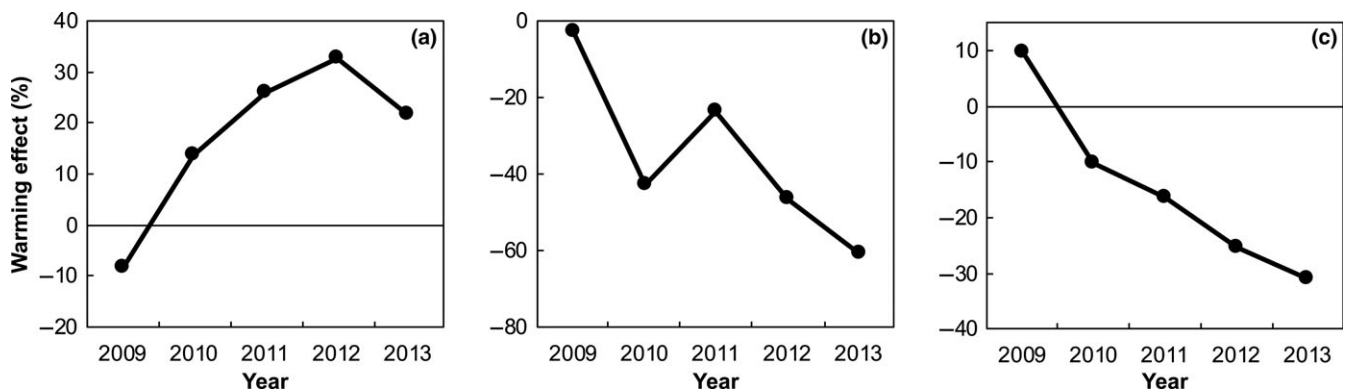
FIGURE 4 Dependence of the warming-induced parameter change on treatment time. (a) Light use efficiency (LUE); (b) baseline turnover rate of the fast SOC pool (k_{fast}); (c) baseline turnover rate of the slow SOC pool (k_{slow})

The parameter changes significantly affected the goodness-of-fit of the model simulations (Figures 5-7). By using the adjusted parameters derived from data assimilation, the simulated GPP, ER, and NEE matched observations well (R^2 from 0.64 to 0.89; Figure 5a–f). Without parameter adjustment, the model performance in the warming treatment was not as good, showing R^2 smaller than 0.6 (Figure 5g–i). Similarly, the model with parameter adjustment showed smaller MAPE in simulating biomass-C (16.9%) than that without parameter adjustment (18.6%) (Figure 6). The MAPE value of SOC was not affected by parameter adjustments (Figure 7).

The altered parameters significantly altered the predicted soil C loss in the Arctic ecosystem (Figure 8). Soil is a C source even under ambient conditions with a cumulative C loss of 69.9 g/m^2 (Figure 8a, d). Without parameter adjustments, warming increased C loss by 321%, reaching a cumulative C loss of 294.2 g/m^2 (Figure 8c, d). With the parameter adjustments from data assimilation, the warming-induced increase in C loss cumulatively reached 156.4 g/m^2 (Figure 8b, d). In summary, the increased C loss with warming was 224.3 and 86.5 g/m^2 without and with parameter

adjustments, respectively. In other words, parameter adjustments resulted in a decrease in the warming-accelerated soil C loss by 61% (Figure 8b, d).

4 | DISCUSSION

4.1 | Biotic responses to warming and changes in model parameters

It has been well-documented that environmental changes can induce a suite of biotic responses, ranging from short-term physiological adjustments (i.e., acclimation) to evolutionary adaptations via changes in the abundances of individual organisms and community assemblages. For example, photosynthesis acclimation to growth temperature has been observed across different species (Berry & Bjorkman, 1980). Acclimation of soil respiration to field warming has also been reported in a tallgrass prairie (Luo et al., 2001). Recent studies have also shown that warming can alter microbial community and functional genes composition in Arctic ecosystems (Hultman et al., 2015; Manzoni et al., 2012).
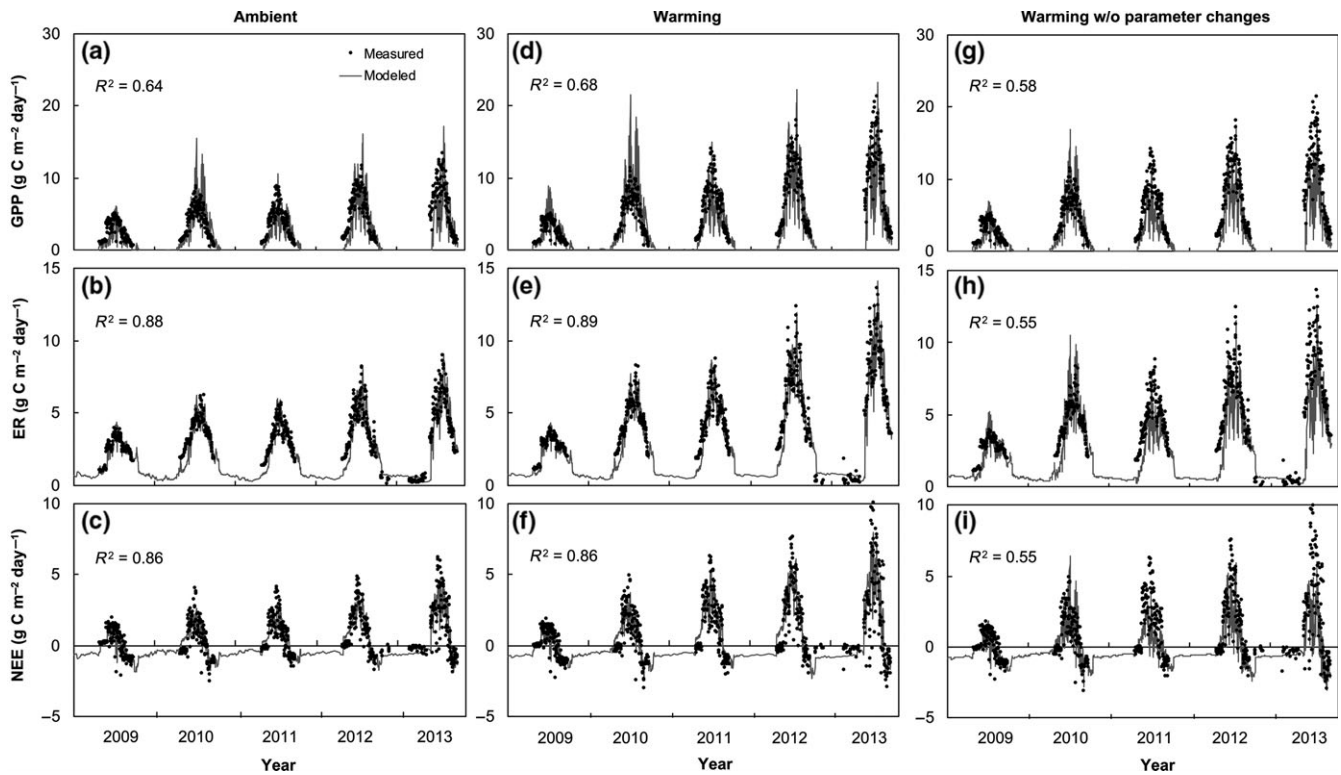
FIGURE 5 Comparison of observed (dots) and model simulated (lines) gross primary production (GPP), ecosystem respiration (ER) and net CO_2 ecosystem exchange (NEE). (a–c), ambient; (d–f), warming; (g–i), warming without parameter adjustments

Physiological acclimation and genetic adaptation fundamentally alter process rates. For example, the optimal temperature of photosynthetic rate (T_{opt}) is adjusted when photosynthesis acclimation occurs under different temperature treatments. Warming-induced increases in the abundance of microbial functional genes for C decomposition also correspond to increases in ecosystem respiration (Natali et al., 2014; Xue et al., 2016). Thus, biotic responses to environmental changes are quantitatively reflected in changes in process rates and, thus in the corresponding model parameter values.

In this study, we used a data assimilation technique to estimate changes of key parameters under soil warming in comparison with those under control conditions at the Eight Mile Lake experimental site of Alaska. Our analyses indicated that the warming treatment significantly increased LUE and decreased the baseline (i.e., environment-corrected) rates of SOC decomposition in both the fast and slow pools (Table 1; Figure 3b, c). In the model, LUE is the efficiency of vegetation in converting the absorbed sunlight to biochemical energy. It is an integrated representation of multiple photosynthetic processes from light-harvesting to C-fixation reactions. Those photosynthetic processes are largely dependent on leaf nitrogen (N) content because of the important roles of N in RuBP carboxylase and chlorophyll (Evans, 1989). Kergoat, Lafont, Arneth, Le Dantec, and Saugier (2008) found that N content controls canopy LUE in a variety of ecosystems. At the CiPEHR site, previous studies have shown that warming and permafrost thaw promotes soil N availability and foliar N pools (Natali et al., 2012; Salmon et al., 2016). Thus, the increased LUE is likely the result of increased plant N acquisition from the soil.

In the model, the baseline turnover rates of the fast and slow pools are the ability of microbial community in decomposing the two SOC pools. They are integrated representations of multiple components and processes, such as the composition of microbial taxa, microbial richness, and microbial activity. Our results showed that warming significantly decreased the baseline rates of SOC decomposition in both the fast and slow pools, possibly due to the microbial acclimation to warming (Bradford et al., 2008; Luo et al., 2001). Consistent with acclimation of the microbial pool to warming, changes in microbial community and functional gene composition have been observed in this study site (Penton et al., 2013; Xue et al., 2016), as well as in other Arctic ecosystems (Deng et al., 2015; Hultman et al., 2015; Manzoni et al., 2012; Yuan et al., 2018). These compositional changes likely have an impact in the decomposition of SOC.

In addition, we explored how other parameters would change if holding baseline turnover rates constant. Results showed that carbon transfer coefficient ($a_{i,j}$, defined as the proportion of carbon from pool j to pool i) among litter and SOC pools increased (Supporting Information Figure S1). In other words, the proportion of carbon from those pools to be respired toward CO_2 release decreased (i.e., increased carbon use efficiency). The results indicate that if baseline turnover rates do not change under warming, the model would increase carbon use efficiency to match data. The increase in carbon use efficiency under warming is another mechanism of acclimation when the baseline turnover rates are constant (Bradford et al., 2008).
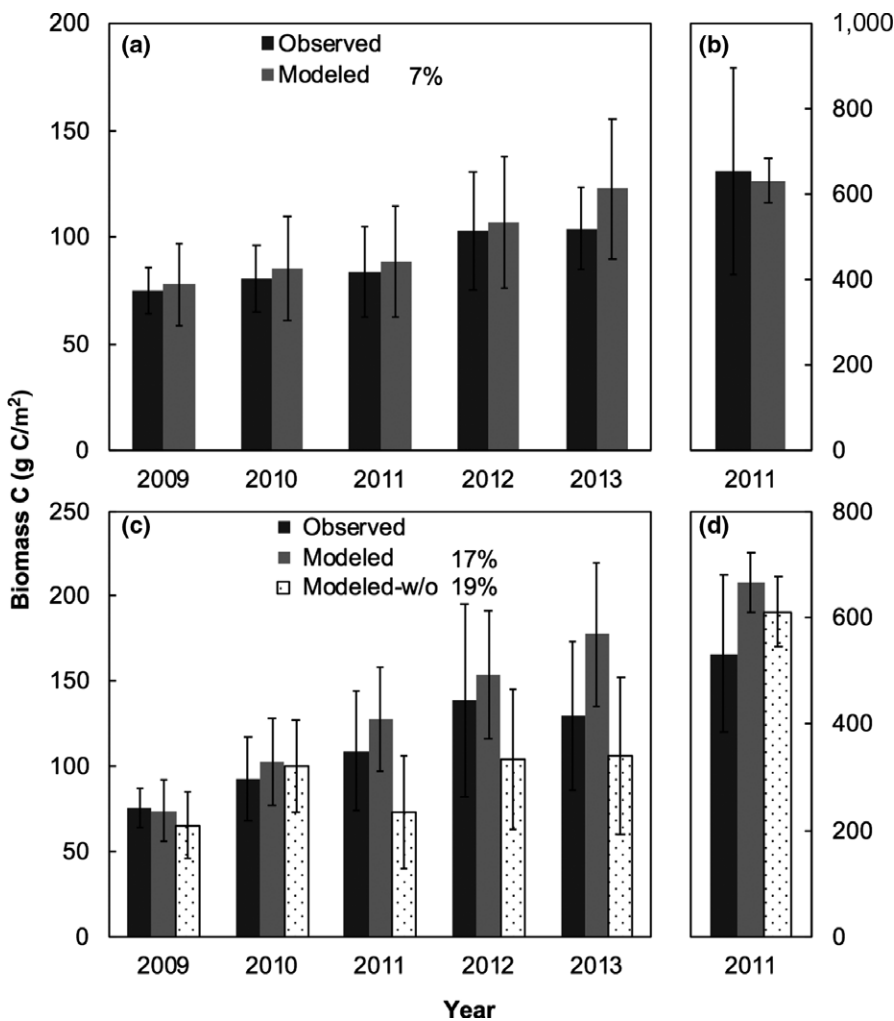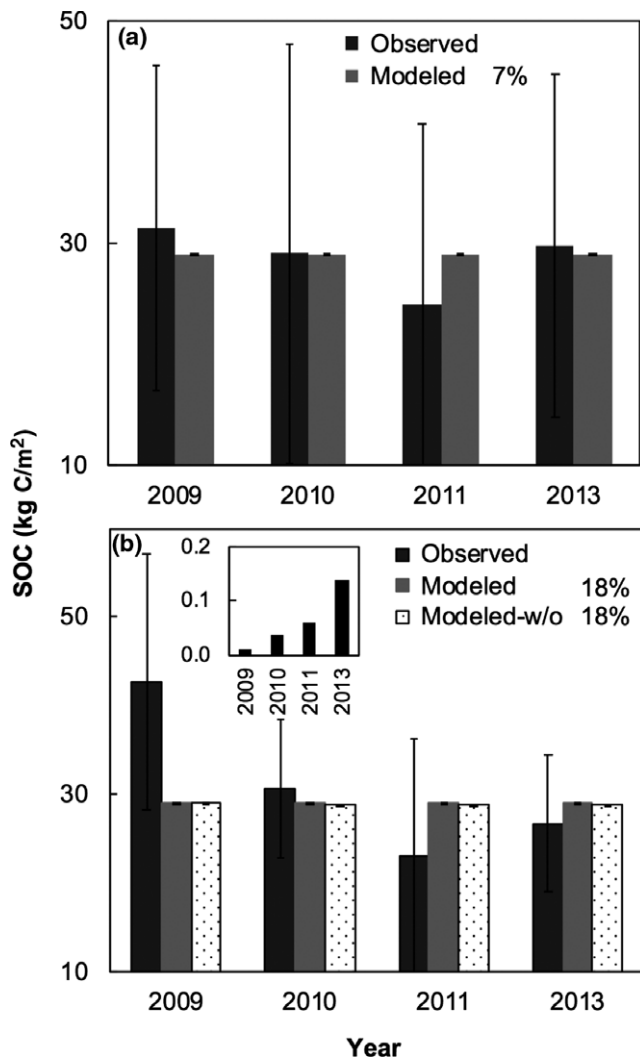
FIGURE 6 Comparison of observed (mean $\pm$ SD) and model simulated aboveground (a, c) and belowground (b, d) biomass-C in the control (a, b) and warming (c, d) treatments. Dot-filled bars in panel c and d are model simulations without parameter adjustments in the warming treatment. Numbers after the legend are corresponding mean absolute percentage errors (MAPE)

Other studies have also demonstrated that global climate change can alter parameter values. For example, assimilation of six data sets into a seven-pool TECO model constrained parameter estimates of the transfer coefficient from the nonwoody biomass pool (i.e., leaf and fine root), resulting in higher coefficients in the elevated than the ambient CO_2 treatment in the Duke Forest Free-Air CO_2 enrichment study (Xu et al., 2006). In another study, 9-year warming decreased the allocation coefficient of GPP to plant shoots as well as the turnover rates of the live C pools (i.e., shoot and root C), but increased the turnover rates of the litter and fast soil C pools in comparison with those under the control treatment in a tallgrass prairie (Shi et al., 2015). Indeed, estimated parameter values related to canopy photosynthesis and ecosystem respiration varied across 12 eddy flux sites and with ecosystem types, and were further correlated with climate variables (Li et al., 2016). Key parameters related to C cycle, such as plant C allocation coefficients have been found to vary spatially across the globe (Bloom, Exbrayat, Van Der Velde, Feng, & Williams, 2016). Thus, regardless of what models are used for data assimilation, it is ubiquitous that model parameters have to adjust in order to fit data well as to reflect biotic responses. In contrast, estimated values do not change much for parameters related to physical processes (Huang et al., 2018).

The variation of biological parameters with global change factors, ecosystem types, and environmental variables reflects a fundamental issue in simulation modeling. A traditional view on simulation modeling is that parameters are constants to represent fundamental properties of a system to be simulated. This definition of parameter may work for physical systems, whereas biological systems constantly evolve over time and with the environment. Thus, parameters to represent biological properties change over time, across space, and with the environment. For example, the optimum temperature has been found to linearly respond to growth temperature for both the maximum rate of carboxylation (Vc_{max}) and the maximum rate of electron transport (J_{max}) (Kattge & Knorr, 2007). However, it has not been explicitly examined in the literature how a varying parameter, e.g., Vc_{max}, can be distinguished from a variable, e.g., canopy photosynthetic rate, for biological systems. This is a critical issue for developing ESMs that can more precisely represent evolutionary processes.

4.2 | Modeled SOC dynamics under changing biotic parameters

Our results showed that warming significantly increased SOC loss to the atmosphere, consistent with previous observational and

FIGURE 7 Comparison of observed and model simulated soil organic carbon (SOC; mean $\pm$ SD) in the control (a) and warming (b) treatments. Dot-filled bars in panel b are model simulations without parameter adjustments in the warming treatment. Numbers after the legend are corresponding mean absolute percentage errors (MAPE). The insert plot shows the difference between the modeled SOC with and without parameter adjustments

modeling studies in permafrost regions (Koven et al., 2011; Mauritz et al., 2017; Natali et al., 2014; Schuur et al., 2015). However, previous modeling studies did not consider warming-induced biotic changes by using fixed model parameters, while field studies usually observe differences between treatments and control and do not separate the respective effects of abiotic versus biotic changes on SOC dynamics. In this study, parameter adjustments significantly improved the model simulated GPP, ER, NEE, and biomass (Figures 5 and 6). This is consistent with previous studies which show improved model performance after parameter adjustments, exhibiting a higher degree of fit between observations and model simulations (Bauer et al., 2015; Shi et al., 2015; Williams et al., 2009; Xu et al., 2006). However, the mean absolute percentage error was not changed for SOC after parameter adjustments (Figure 7). This may be because that the SOC stock in this study site was large and had

relatively wide range of variation due to heterogeneity (29762.2 $\pm$ 18505.0 g/m^2; mean $\pm$ SD across treatments and years). The modeled SOC stock, with or without parameter adjustments, fell within the wide observed range (Figure 7). In comparison to the total SOC stock, the magnitude of SOC changes induced by parameter adjustments (11.8, 37.0, 58.5, and 137.8 g/m^2 for 2009, 2010, 2011, and 2013, respectively) was much smaller for the 5-year experiment. Thus, when looking at the total SOC stocks, the modeled values were similar with or without parameter adjustments. As a result, the calculated mean absolute percentage error was not changed for total SOC stock by the parameter adjustments. The simulation of SOC stock may be further improved by increasing its weight in the cost function.

Although the SOC change induced by parameter adjustments was not very large in comparison with the total stock, it may have remarkable impacts on the land-atmosphere C balance and climate change on long-term scales. In this study, parameter adjustments resulted in a 61% reduction of warming-induced CO_2 emission from SOC to the atmosphere, indicating that the current generation of ESMs, which primarily utilize fixed model parameters, may overestimate SOC loss in Arctic ecosystems. In addition, the impact of parameter adjustments on SOC may be observed with longer term experiments. For example, parameter adjustments significantly improved the simulation of SOC in a 10-year experiment in a tallgrass prairie (Shi et al., 2015).

Process-based land models have been widely implemented to help understand ecosystem responses to climate warming (Cox, Betts, Jones, Spall, & Totterdell, 2000; Eliasson et al., 2005; Knorr, Prentice, House, & Holland, 2005). The majority of the models include processes related to plant physiology, phenology, and soil C dynamics. Parameterization of the physiological responses to warming usually implements some temperature response functions with an optimum temperature ranging from 20 to 40°C for most models, e.g., CLM4.5 (Oleson et al., 2013), LPJ (Sitch et al., 2003), LPJ-GUESS (Smith et al., 2014), JULES (Clark et al., 2011), ORCHIDEE (Krinner et al., 2005), TECO (Weng & Luo, 2008), and CABLE (Kowalczyk et al., 2006). In the permafrost region where the mean annual growing season temperature is much lower than 20°C, those models are likely to exhibit an increased photosynthetic rate under warming conditions. Phenological responses to warming, such as changes in leaf onset dates, are parameterized with an accumulated temperature, e.g., growing degree days (GDDs), for most models, including CLM4.5, G'DAY (Botta, Viovy, Ciais, Friedlingstein, & Monfray, 2000), ISAM (Song, Jain, & Mcisaac, 2013), LPJ (Sitch et al., 2003), LPJ-GUESS (Smith et al., 2014), O-CN (Krinner et al., 2005), ORCHIDEE (Krinner et al., 2005), SDGVM (Woodward & Lomas, 2004), and TECO (Weng & Luo, 2008). Warming usually has leaf onset earlier and extends the growing season length. Accordingly, most models likely simulate a positive warming response on vegetation productivity in the permafrost region. The positive responses simulated by those processes-based models may partially translate to the increased LUE in this study. This elevated LUE can increase plant CO_2 assimilation, partially alleviating the positive feedback of Arctic C cycling to climate change (Mauritz et al., 2017; Natali et al., 2012).
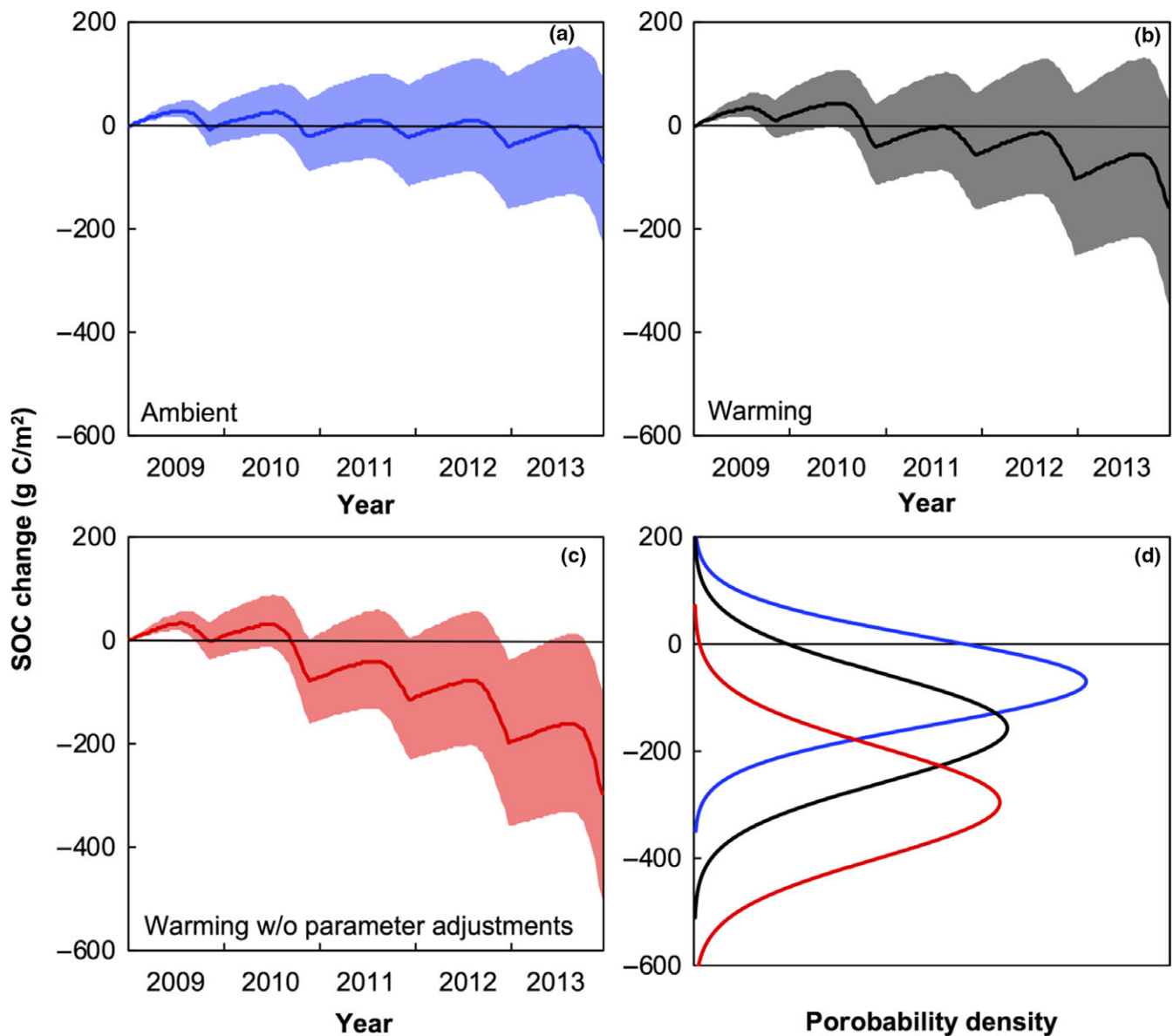
FIGURE 8 Model simulated SOC change from 2009 to 2013 under different conditions. (a) Ambient; (b) warming; (c) warming without parameter adjustments; (d) distribution of the cumulative SOC change under the three scenarios. (a–c) The solid line and the shading area are the mean and 95% confidence interval. (d) Line colors are corresponding to that in a–c

However, the estimated changes in SOC pool baseline turnover rates in this study may not be reproducible by many of the land models that follow a similar structure of first-order kinetics of C transfer among multiple pools, as in the CENTURY model (Parton, Schimel, Cole, & Ojima, 1987; Parton, Stewart, & Cole, 1988). In the current generation of ESMs with fixed parameters, the responses of soil respiration to warming are mostly controlled by temperature response functions such as, the Q_{10} exponential temperature or Arrhenius functions (Lloyd & Taylor, 1994). Thus, modeled warming effects on the decomposition of SOC pools do not include biotic responses. The data assimilation result from this study, which is the warming-induced decrease in baseline soil C turnover rates, can be hardly represented by the current generation of ESMs no matter how complex those models are. As a consequence, without

considering warming-induced changes in soil C turnover rates, ESMs may overestimate the loss of soil C.

4.3 | Incorporation of biotic responses into ESMs

Biotic responses to global change have been recognized to strongly influence modeling results (Atkin et al., 2008; Friend, 2010; Lombardozzi, Bonan, Smith, Dukes, & Fisher, 2015; Ziehn, Kattge, Knorr, & Scholze, 2011). Studies have been performed that incorporate different types of biotic responses into models. For example, plant photosynthetic and respiratory acclimation to temperature has been integrated into an ecosystem model (Friend, 2010). This model allowed the optimum temperature for J_{max} to respond to changes in plant growth temperature by assuming the optimum leaf

temperature linearly decays toward an equilibrium temperature. In addition, several other studies have also been performed to incorporate plant photosynthetic and/or respiratory acclimation into ESMs (Atkin et al., 2008; Lombardozzi et al., 2015; Ziehn et al., 2011).

However, it is much more difficult to incorporate microbial acclimation and adaptation than plant acclimation into ESMs since estimated shifts in rates of SOC decomposition in response to warming may involve multiple mechanisms such as the thermal acclimation of microbial respiration (enzyme conformation and isozyme production) and adaptations due to changes in microbial community composition. Most of those microbial processes are not very well resolved at the scales of explicit model structure representation. Nevertheless, recent studies have attempted to add explicit microbial pools in models (Allison, Wallenstein, & Bradford, 2010; Wang, Post, & Mayes, 2013; Wieder, Bonan, & Allison, 2013). Models with explicit microbial pools usually use Michaelis–Menten or reverse Michaelis–Menten equations to represent microbial substrate assimilation and decomposition. Although some of the microbial models were initially intended to represent microbial acclimation, it is not yet clear how well the models can achieve it. Moreover, these nonlinear microbial models behave unrealistically when simulating soil C dynamics (Wang et al., 2014) and still lack empirical evidence for support.

Alternatively, those unresolved microbial processes are represented by changes in parameter values in association with physiological acclimation and genetic adaptation using data assimilation techniques. The estimated shifts in model parameters are at least grounded in observations. In this study, we show that three key parameters shifted under the warming treatment in comparison with the control. Parameter changes also strongly depend on treatment time, indicating that warming-induced biological changes are gradual instead of step changes (Figure 4), as exposure time to environmental stimuli can affect the extent to which acclimation occurs (Smith & Dukes, 2013). The gradual shifts in parameter values are likely due to time-dependent adjustments in physiological processes and microbial composition. Additionally, it is reasonable to assume that model parameter changes are also dependent on the magnitudes of environmental stimuli (temperature increase and permafrost thaw). Thus, model parameters need to be updated frequently to represent biological changes such as the acclimation of photosynthesis, autotrophic respiration and heterotrophic respiration to warming.

While this study estimated site- and treatment-specific changes in parameters, general patterns of parameter changes across different environmental conditions and ecosystem types has been recently explored (Li et al., 2016). Searching for general patterns of parameter changes certainly needs more research in the future. Nevertheless, the concept of adjusting parameters to match model with data well is generally applicable to all model-data integration studies.

ORCID

Junyi Liang http://orcid.org/0000-0001-8252-5502
Jiangyang Xia http://orcid.org/0000-0001-5923-6665
Zheng Shi http://orcid.org/0000-0002-5067-9977
Xingjie Lu http://orcid.org/0000-0003-3732-1978
Marguerite Mauritz http://orcid.org/0000-0001-8733-9119
Verity G. Salmon http://orcid.org/0000-0002-2188-551X

REFERENCES

Allison, S. D., Wallenstein, M. D., & Bradford, M. A. (2010). Soil-carbon response to warming dependent on microbial physiology. *Nature Geoscience*, *3*, 336–340. https://doi.org/10.1038/ngeo846

Atkin, O. K., Atkinson, L. J., Fisher, R. A., Campbell, C. D., Zaragoza-Castells, J., Pitchford, J. W., . . . Hurry, V. (2008). Using temperature-dependent changes in leaf scaling relationships to quantitatively account for thermal acclimation of respiration in a coupled global climate–vegetation model. *Global Change Biology*, *14*, 2709–2726.

Bauer, P., Thorpe, A., & Brunet, G. (2015). The quiet revolution of numerical weather prediction. *Nature*, *525*, 47–55. https://doi.org/10.1038/nature14956

Berry, J., & Bjorkman, O. (1980). Photosynthetic response and adaptation to temperature in higher plants. *Annual Review of plant physiology*, *31*, 491–543. https://doi.org/10.1146/annurev.pp.31.060180.002423

Bloom, A. A., Exbrayat, J.-F., Van Der Velde, I. R., Feng, L., & Williams, M. (2016). The decadal state of the terrestrial carbon cycle: Global retrievals of terrestrial carbon allocation, pools, and residence times. *Proceedings of the National Academy of Sciences*, *113*, 1285–1290. https://doi.org/10.1073/pnas.1515160113

Botta, A., Viovy, N., Ciais, P., Friedlingstein, P., & Monfray, P. (2000). A global prognostic scheme of leaf onset using satellite data. *Global Change Biology*, *6*, 709–725. https://doi.org/10.1046/j.1365-2486.2000.00362.x

Bracho, R., Natali, S., Pegoraro, E., Crummer, K. G., Schädel, C., Celis, G., . . . Schuur, E. A. G. (2016). Temperature sensitivity of organic matter decomposition of permafrost-region soils during laboratory incubations. *Soil Biology and Biochemistry*, *97*, 1–14. https://doi.org/10.1016/j.soilbio.2016.02.008

Bradford, M. A., Davies, C. A., Frey, S. D., Maddox, T. R., Melillo, J. M., Mohan, J. E., . . . Wallenstein, M. D. (2008). Thermal adaptation of soil microbial respiration to elevated temperature. *Ecology Letters*, *11*, 1316–1327. https://doi.org/10.1111/j.1461-0248.2008.01251.x

Carvalhais, N., Reichstein, M., Collatz, G. J., Pereira, J. S., Berbigier, P., Carrara, A., . . . Valentini, R. (2008). Implications of the carbon cycle steady state assumption for biogeochemical modeling performance and inverse parameter retrieval. *Global Biogeochemical Cycles*, *22*, https://doi.org/10.1029/2007GB003033

Clark, D. B., Mercado, L. M., Sitch, S., Jones, C. D., Gedney, N., Best, M. J., . . . Cox, P. M. (2011). The Joint UK Land Environment Simulator (JULES), model description - Part 2: Carbon fluxes and vegetation dynamics. *Geoscientific Model Development*, *4*, 701–722. https://doi.org/10.5194/gmd-4-701-2011

Cox, P. M., Betts, R. A., Jones, C. D., Spall, S. A., & Totterdell, I. J. (2000). Acceleration of global warming due to carbon-cycle feedbacks in a coupled climate model. *Nature*, 408, 184–187. https://doi.org/10.1038/35041539

Davidson, E. A., & Janssens, I. A. (2006). Temperature sensitivity of soil carbon decomposition and feedbacks to climate change. *Nature*, 440, 165–173. https://doi.org/10.1038/nature04514

Deng, J., Gu, Y. F., Zhang, J., Xue, K., Qin, Y., Yuan, M., . . . Zhou, J. (2015). Shifts of tundra bacterial and archaeal communities along a permafrost thaw gradient in Alaska. *Molecular Ecology*, 24, 222–234. https://doi.org/10.1111/mec.13015

Eliasson, P. E., Mcmurtrie, R. E., Pepper, D. A., Stromgren, M., Linder, S., & Agren, G. I. (2005). The response of heterotrophic CO_2 flux to soil warming. *Global Change Biology*, 11, 167–181. https://doi.org/10.1111/j.1365-2486.2004.00878.x

Evans, J. R. (1989). Photosynthesis and nitrogen relationships in leaves of C-3 plants. *Oecologia*, 78, 9–19. https://doi.org/10.1007/BF00377192

Friend, A. D. (2010). Terrestrial plant production and climate change. *Journal of Experimental Botany*, 61, 1293–1309. https://doi.org/10.1093/jxb/erq019

Gelman, A., Roberts, G., & Gilks, W. (1996). Efficient metropolis jumping hules. *Bayesian Statistics*, 5, 599–607.

Haario, H., Saksman, E., & Tamminen, J. (2001). An adaptive metropolis algorithm. *Bernoulli*, 7, 223–242.

Hararuk, O., Xia, J., & Luo, Y. (2014). Evaluation and improvement of a global land model against soil carbon data using a Bayesian Markov chain Monte Carlo method. *Journal of Geophysical Research: Biogeosciences*, 119, 403–417.

Hicks Pries, C. E., Schuur, E.A.G., Natali, S. M., & Crummer, K. G. (2016). Old soil carbon losses increase with ecosystem respiration in experimentally thawed tundra. *Nature Climate Change*, 6, 214–218. https://doi.org/10.1038/nclimate2830

Huang, Y., Lu, X., Lawrence, D., Koven, C. D., Xia, J., Du, X., . . . Luo, Y. (2018). Matrix approach to land carbon cycle modeling: A case study with the Community Land Model. *Global Change Biology*, 24, 1394–1404. https://doi.org/10.1111/gcb.13948

Hultman, J., Waldrop, M. P., Mackelprang, R., David, M. M., McFarland, J., Blazewicz, S. T., . . . Jansson, J. K. (2015). Multi-omics of permafrost, active layer and thermokarst bog soil microbiomes. *Nature*, 521, 208–212. https://doi.org/10.1038/nature14238

Kattge, J., & Knorr, W. (2007). Temperature acclimation in a biochemical model of photosynthesis: A reanalysis of data from 36 species. *Plant, Cell & Environment*, 30, 1176–1190. https://doi.org/10.1111/j.1365-3040.2007.01690.x

Keenan, T. F., Davidson, E. A., Munger, J. W., & Richardson, A. D. (2013). Rate my data: Quantifying the value of ecological data for the development of models of the terrestrial carbon cycle. *Ecological Applications*, 23, 273–286. https://doi.org/10.1890/12-0747.1

Kergoat, L., Lafont, S., Arneth, A., Le Dantec, V., & Saugier, B. (2008). Nitrogen controls plant canopy light-use efficiency in temperate and boreal ecosystems. *Journal of Geophysical Research-Biogeosciences*, 113, G04017. https://doi.org/10.1029/2007JG000676

Knorr, W., Prentice, I. C., House, J. I., & Holland, E. A. (2005). Long-term sensitivity of soil carbon turnover to warming. *Nature*, 433, 298–301. https://doi.org/10.1038/nature03226

Koven, C. D., Lawrence, D. M., & Riley, W. J. (2015). Permafrost carbon−climate feedback is sensitive to deep soil carbon decomposability but not deep soil nitrogen dynamics. *Proceedings of the National Academy of Sciences*, 112, 3752–3757.

Koven, C. D., Riley, W. J., & Stern, A. (2013). Analysis of permafrost thermal dynamics and response to climate change in the CMIP5 earth system models. *Journal of Climate*, 26, 1877–1900. https://doi.org/10.1175/JCLI-D-12-00228.1

Koven, C. D., Ringeval, B., Friedlingstein, P., Ciais, P., Cadule, P., Khvorostyanov, D., . . . Tarnocai, C. (2011). Permafrost carbon-climate feedbacks accelerate global warming. *Proceedings of the National Academy of Sciences of the United States of America*, 108, 14769–14774. https://doi.org/10.1073/pnas.1103910108

Kowalczyk, E., Wang, Y. P., Law, R. M., Davies, H. L., Mcgregor, J. L., & Abramowitz, G. (2006). The CSIRO Atmosphere Biosphere Land Exchange (CABLE) model for use in climate models and as an offline model (ed Commonw. Sci. And Ind. Res. Organ. Mar. And Atmos. Res. A, Vic., Australia) pp Page.

Krinner, G., Viovy, N., De Noblet-Ducoudre, N., Ogée, J., Polcher, J., Friedlingstein, P., . . . Prentice, I. C. (2005). A dynamic global vegetation model for studies of the coupled atmosphere-biosphere system. *Global Biogeochemical Cycles*, 19, GB1015. https://doi.org/10.1029/2003GB002199

Li, Q. Y., Xia, J. Y., Shi, Z., Huang, K., Du, Z. G., Lin, G. H., & Luo, Y. Q. (2016). Variation of parameters in a Flux-Based Ecosystem Model across 12 sites of terrestrial ecosystems in the conterminous USA. *Ecological Modelling*, 336, 57–69. https://doi.org/10.1016/j.ecolmodel.2016.05.016

Liang, J. Y., Li, D. J., Shi, Z., Tiedje, J. M., Zhou, J., Schuur, E. A. G., . . . Luo, Y. (2015). Methods for estimating temperature sensitivity of soil organic matter based on incubation data: A comparative evaluation. *Soil Biology & Biochemistry*, 80, 127–135. https://doi.org/10.1016/j.soilbio.2014.10.005

Lloyd, J., & Taylor, J. A. (1994). On the temperature-dependence of soil respiration. *Functional Ecology*, 8, 315–323. https://doi.org/10.2307/2389824

Lombardozzi, D. L., Bonan, G. B., Smith, N. G., Dukes, J. S., & Fisher, R. A. (2015). Temperature acclimation of photosynthesis and respiration: A key uncertainty in the carbon cycle-climate feedback. *Geophysical Research Letters*, 42, 8624–8631. https://doi.org/10.1002/2015GL065934

Luo, Y., Ahlström, A., Allison, S. D., Batjes, N. H., Brovkin, V., Carvalhais, N., . . . Georgiou, K. (2016). Toward more realistic projections of soil carbon dynamics by Earth system models. *Global Biogeochemical Cycles*, 30, 40–56. https://doi.org/10.1002/2015GB005239

Luo, Y., Ogle, K., Tucker, C., Fei, S., Gao, C., LaDeau, S., . . . Schimel, D. S. (2011). Ecological forecasting and data assimilation in a data-rich era. *Ecological Applications*, 21, 1429–1442. https://doi.org/10.1890/09-1275.1

Luo, Y., Shi, Z., Lu, X., Xia, J., Liang, J., Jiang, J., . . . Wang, Y.-P. (2017). Transient dynamics of terrestrial carbon storage: Mathematical foundation and its applications. *Biogeosciences*, 14, 145. https://doi.org/10.5194/bg-14-145-2017

Luo, Y., Wan, S., Hui, D., & Wallace, L. L. (2001). Acclimatization of soil respiration to warming in a tall grass prairie. *Nature*, 413, 622–625. https://doi.org/10.1038/35098065

Macdougall, A. H., Avis, C. A., & Weaver, A. J. (2012). Significant contribution to climate warming from the permafrost carbon feedback. *Nature Geoscience*, 5, 719–721. https://doi.org/10.1038/ngeo1573

Manzoni, S., Taylor, P., Richter, A., Porporato, A., & Ägren, G. I. (2012). Environmental and stoichiometric controls on microbial carbon-use efficiency in soils. *New Phytologist*, 196, 79–91. https://doi.org/10.1111/j.1469-8137.2012.04225.x

Mauritz, M., Bracho, R., Celis, G., Hutchings, J., Natali, S. M., Pegoraro, E., . . . Schuur, E. A. G. (2017). Nonlinear CO2 flux response to 7 years of experimentally induced permafrost thaw. *Global Change Biology*, 23, 3646–3666. https://doi.org/10.1111/gcb.13661

Mcguire, A. D., Christensen, T. R., Hayes, D., Heroult, A., Euskirchen, E., Yi, Y., . . . Kimball, M. (2012). An assessment of the carbon balance of Arctic tundra: Comparisons among observations, process models, and atmospheric inversions. *Biogeosciences*, 9, 3185–3204. https://doi.org/10.5194/bg-9-3185-2012

Mcguire, A. D., Koven, C., Lawrence, D. M., Clein, J. S., Xia, J., Beer, C., . . . Zhuang, Q. (2016). Variability in the sensitivity among model simulations of permafrost and carbon dynamics in the permafrost region

between 1960 and 2009. *Global Biogeochemical Cycles*, 30, 1015–1037. https://doi.org/10.1002/2016GB005405

Natali, S. M., Schuur, E.A.G., & Rubin, R. L. (2012). Increased plant productivity in Alaskan tundra as a result of experimental warming of soil and permafrost. *Journal of Ecology*, 100, 488–498. https://doi.org/10.1111/j.1365-2745.2011.01925.x

Natali, S. M., Schuur, E.A.G., Trucco, C., Pries, C. E. H., Crummer, K. G., & Lopez, A. F. B. (2011). Effects of experimental warming of air, soil and permafrost on carbon balance in Alaskan tundra. *Global Change Biology*, 17, 1394–1407. https://doi.org/10.1111/j.1365-2486.2010.02303.x

Natali, S. M., Schuur, E.A.G., Webb, E. E., Pries, C. E. H., & Crummer, K. G. (2014). Permafrost degradation stimulates carbon loss from experimentally warmed tundra. *Ecology*, 95, 602–608. https://doi.org/10.1890/13-0602.1

Oleson, K. W., Lawrence, D. M., Bonan, G. B., Bonan, G. B., Drewiak, B., Huang, M., . . . Thornton, P. E. (2013). Technical Description of Version 4.5 of the Community Land Model (CLM). pp Page, NCAR Technical Note NCAR/TN-503 + STR, Boulder, Colorado.

Parton, W. J., Schimel, D. S., Cole, C. V., & Ojima, D. S. (1987). Analysis of factors controlling soil organic-matter levels in great-plains grasslands. *Soil Science Society of America Journal*, 51, 1173–1179. https://doi.org/10.2136/sssaj1987.03615995005100050015x

Parton, W. J., Stewart, J. W. B., & Cole, C. V. (1988). Dynamics of C, N, P and S in grassland soils - a model. *Biogeochemistry*, 5, 109–131. https://doi.org/10.1007/BF02180320

Penton, C. R., St Louis, D., Luo, Y., Wu, L., Schuur, E. A. G., Zhou, J., & Tiedje, J. M. (2013). Fungal diversity in permafrost and tallgrass prairie soils under experimental warming conditions. *Applied and Environmental Microbiology*, 79, 7063–7072. https://doi.org/10.1128/AEM.01702-13

Salmon, V. G., Soucy, P., Mauritz, M., Celis, G., Natali, S. M., Mack, M. C., & EaG, S. (2016). Nitrogen availability increases in a tundra ecosystem during five years of experimental permafrost thaw. *Global Change Biology*, 22, 1927–1941. https://doi.org/10.1111/gcb.13204

Schuur, E. A. G., Mcguire, A. D., Schadel, C., Grosse, G., Harden, J. W., Hayes, D. J., . . . Natali, S. (2015). Climate change and the permafrost carbon feedback. *Nature*, 520, 171–179. https://doi.org/10.1038/nature14338

Schuur, E.A.G., Vogel, J. G., Crummer, K. G., Lee, H., Sickman, J. O., & Osterkamp, T. E. (2009). The effect of permafrost thaw on old carbon release and net carbon exchange from tundra. *Nature*, 459, 556–559. https://doi.org/10.1038/nature08031

Shi, Z., Xu, X., Hararuk, O., Jiang, L., Xia, J., Liang, J., . . . Luo, Y. (2015). Experimental warming altered rates of carbon processes, allocation, and carbon storage in a tallgrass prairie. *Ecosphere*, 6, 1–16.

Sitch, S., Smith, B., Prentice, I. C., Arneth, A., Bondeau, A., Cramer, W., . . . Venevsky, S. (2003). Evaluation of ecosystem dynamics, plant geography and terrestrial carbon cycling in the LPJ dynamic global vegetation model. *Global Change Biology*, 9, 161–185. https://doi.org/10.1046/j.1365-2486.2003.00569.x

Smith, N. G., & Dukes, J. S. (2013). Plant respiration and photosynthesis in global-scale models: Incorporating acclimation to temperature and CO_2. *Global Change Biology*, 19, 45–63. https://doi.org/10.1111/j.1365-2486.2012.02797.x

Smith, B., Warlind, D., Arneth, A., Hickler, T., Leadley, P., Siltberg, J., & Zaehle, S. (2014). Implications of incorporating N cycling and N limitations on primary production in an individual-based dynamic vegetation model. *Biogeosciences*, 11, 2027–2054. https://doi.org/10.5194/bg-11-2027-2014

Song, Y., Jain, A. K., & Mcisaac, G. F. (2013). Implementation of dynamic crop growth processes into a land surface model: Evaluation of energy, water and carbon fluxes under corn and soybean rotation.

Biogeosciences, 10, 8039–8066. https://doi.org/10.5194/bg-10-8039-2013

Wang, Y. P., Chen, B. C., Wieder, W. R., Leite, M., Medlyn, B. E., Rasmussen, M., . . . Luo, Q. (2014). Oscillatory behavior of two nonlinear microbial models of soil carbon decomposition. *Biogeosciences*, 11, 1817–1831. https://doi.org/10.5194/bg-11-1817-2014

Wang, G., Post, W. M., & Mayes, M. A. (2013). Development of microbial-enzyme-mediated decomposition model parameters through steady-state and dynamic analyses. *Ecological Applications*, 23, 255–272. https://doi.org/10.1890/12-0681.1

Webb, E. E., Schuur, E.A.G., Natali, S. M., Oken, K. V., Bracho, R., Krapek, J. P., . . . Nickerson, N. R. (2016). Increased wintertime CO_2 loss as a result of sustained tundra warming. *Journal of Geophysical Research-Biogeosciences*, 121, 249–265. https://doi.org/10.1002/2014JG002795

Weng, E. S., & Luo, Y. Q. (2008). Soil hydrological properties regulate grassland ecosystem responses to multifactor global change: A modeling analysis. *Journal of Geophysical Research-Biogeosciences*, 113, G03003. https://doi.org/10.1029/2007JG000539

Weng, E., & Luo, Y. (2011). Relative information contributions of model vs. data to short- and long-term forecasts of forest carbon dynamics. *Ecological Applications*, 21, 1490–1505. https://doi.org/10.1890/09-1394.1

Wieder, W. R., Bonan, G. B., & Allison, S. D. (2013). Global soil carbon projections are improved by modelling microbial processes. *Nature Clim. Change*, 3, 909–912. https://doi.org/10.1038/nclimate1951

Williams, M., Richardson, A., Reichstein, M., Stoy, P. C., Peylin, P., Verbeeck, H., . . . Wang, Y.-P. (2009). Improving land surface models with FLUXNET data. *Biogeosciences*, 6, 1341–1359. https://doi.org/10.5194/bg-6-1341-2009

Woodward, F. I., & Lomas, M. R. (2004). Vegetation dynamics - simulating responses to climatic change. *Biological Reviews*, 79, 643–670. https://doi.org/10.1017/S1464793103006419

Xu, T., White, L., Hui, D., & Luo, Y. (2006). Probabilistic inversion of a terrestrial ecosystem model: Analysis of uncertainty in parameter estimation and model prediction. *Global Biogeochemical Cycles*, 20, GB2007. https://doi.org/10.1111/gcb.13820

Xue, K., Yuan, M. M., Shi, Z. J., Qin, Y., Deng, Y., Cheng, L., . . . Zhou, J. (2016). Tundra soil carbon is vulnerable to rapid microbial decomposition under climate warming. *Nature Climate Change*, 6, 595–600.

Yuan, M. M. M., Zhang, J., Xue, K., Wu, L., Deng, Y., Deng, J., . . . Zhou, J. (2018). Microbial functional diversity covaries with permafrost thaw-induced environmental heterogeneity in tundra soil. *Global Change Biology*, 24, 297–307.

Ziehn, T., Kattge, J., Knorr, W., & Scholze, M. (2011). Improving the predictability of global CO_2 assimilation rates under climate change. *Geophysical Research Letters*, 38, L10404.

SUPPORTING INFORMATION

Additional supporting information may be found online in the Supporting Information section at the end of the article.